

SYNTHESIS OF SUBMICRONIC α -ALUMINA FROM LOCAL ALUMINUM SLAGS

A. Benkhelif^{a,b}, M. Kolli^{a,b}, M. Hamidouche^{a,b,c,*}

^a Ferhat Abbas Setif 1 University, Research Unit of Emergent Materials, Setif, Algeria

^b Ferhat Abbas Setif 1 University, Institute of Optics and Precision Mechanics, Setif, Algeria

^c Research Center in Industrial Technologies CRTI, B.P. 64, Cheraga 16014, Algiers, Algeria

(Received 01 April 2021; accepted 18 November 2021)

Abstract

In this study, a high valued product submicronic α -alumina was successfully extracted from aluminum slags generated by the local aluminum industry. The extraction technique was based on the leaching of slags by H_2SO_4 followed by precipitation. The coarser aluminum-rich fractions of the slags were used in this study instead of the finer oxide-rich fractions that were commonly used in previous studies. The precipitation of the leached slags by NH_4OH was controlled by a zetameter in order to determine the optimal precipitation pH. Then, the obtained gel showing the higher precipitation rate and the finer particle size was calcined at 1200 °C and characterized by the XRF, XRD, FTIR, SEM, EDS, and laser granulometry. Even without any pretreatment of slags, the XRF analysis revealed that a high purity and high extraction efficiency of 99.2% and 93.75% respectively could be achieved just at a leaching acid concentration of 15%. The XRD spectrum shows that the produced alumina was pure α -corundum, which was confirmed by the FTIR spectrum showing only the Al-O bonds. The laser granulometry showed that the recovered powder exhibited a wide particle size distribution, which was between 50 nm and 20 μ m, while the average particle size (d_{50}) was about 400 nm. The SEM observations revealed that the grains were in the form of submicronic whiskers. The above characteristics allowed the obtained alumina powder in this study to be used in the usual applications of alumina such as refractory, ceramic fibers, abrasive, etc. The obtained powders may also assume applications as a thermally stable substitute for the commonly used transition alumina powders, which needs further investigations in future studies.

Keywords: α -alumina; Aluminum slags; Acid leaching; Precipitation; Calcination

1. Introduction

Alumina is a compound that exhibits several phases like α , γ , β , and θ , etc. [1], while the most stable phase is α -alumina with very interesting properties such as high hardness, high melting temperature, chemical stability, and high elastic modulus [1–4]. Moreover, the combination of a high thermal coefficient, low thermal expansion, and high compressive strength provides α -alumina a good resistance to thermal shock [1, 5]. All these important properties make α -alumina a material in demand in a wide variety of fields. It is used to produce refractory ceramics, high-strength ceramics, abrasives and other ceramic materials [2, 4]. Submicronic and Nano-sized α -alumina powders are also in demand in the field of catalysis as a thermally stable alternative to the widely used transition alumina powders that undergo phase

transformations when used at high temperatures [6].

Submicronic α -alumina powders can be produced by a wide variety of synthesis processes, including sol-gel [7], chemical synthesis [8], laser ablation [9], hydrolysis [10], thermal decomposition [11], and chemical vapor deposition [12], etc. However, these methods involve the use of relatively expensive raw materials such as aluminum sulfates [13]. It is, therefore, of great importance to find inexpensive alternative raw materials. One of the most important inexpensive sources from which we can obtain raw materials to produce α -alumina powder is the treatment of aluminum industries wastes. As aluminum transformation industries can produce large quantities of aluminum slags, which is a waste material formed on the surface of molten aluminum and exposed to the atmosphere during the melting process. These slags contain many important

* Corresponding author: hamidouchemohamed@yahoo.fr



components such as aluminum (12–20%), sodium chloride (20–25%), potassium chloride (20–25%), aluminum oxides (20–50%), and other compounds (2–5%) [14]. On the other hand, as these slags have been classified as toxic waste, its disposal at a garbage dump is prohibited in many countries [15]. For this reason, the subject of recycling these wastes to eliminate their toxicity is of great interest. Accordingly, many studies have addressed the issue of the recycling and valorization of aluminum slags. Direct applications as raw materials in the refractory brick [16] or in the production of inert filling for construction, road paving, mortar components, polymer composites, adsorbents, and mineral wool have been reported [17], while other researchers have aimed to use them to manufacture other raw materials, such as hydrogen gas [18], X-zeolites [19], aluminum sulfate ($\text{Al}_2(\text{SO}_4)_3 \cdot 18\text{H}_2\text{O}$) [20], and alumina with different properties for many applications like catalysis [21,22], cement [23], biomaterials [24], and refractory [16].

In this study, a novel process was developed to recover alumina from aluminum slags. This process is based on acid leaching of the slags followed by alkaline precipitation. The coarse fraction of the slags, which is rich in aluminum, is used directly without any pretreatment instead of the finer oxide-rich fraction commonly used in other studies. The process involves several steps: selective crushing and sieving in order to recover the maximum aluminum compounds present in the slags, leaching in different concentrations of sulphuric acid (H_2SO_4), purification, precipitation by the addition of different amounts of ammonia varying the pH of the suspension between 4 and 10, filtration, drying, and calcination. The study is assisted by the XRF, XRD, FTIR, SEM, EDS, and laser granulometry characterizations in order to optimize the extraction conditions, namely, the leaching acid concentration and the precipitation pH for recovering the maximum amount of alumina with the maximum purity and with well-known morphology and particle size distribution. The main objectives of the present study are to eliminate the harmful effect of aluminum slags on the environment and to provide the local ceramic industry with a very high value-added raw material that is submicronic α -alumina powder.

2. Experimental procedure

2.1. Raw materials

The aluminum slags used in this work were collected from a local aluminum transformer “El Ashir Min Ramadan”. The crushed slags had inherent heterogeneity for aluminum compounds concentrate in the coarser fractions, while oxide and non-metallic compounds accumulated in the finer fractions. This

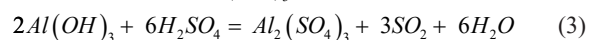
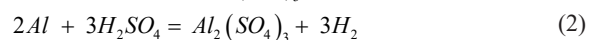
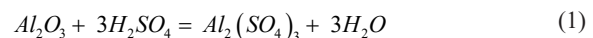
occurred because aluminum behaved plastically and remained unfragmented, while oxides and salts were brittle and fragmented easily [17, 25]. A sieving of the above-mentioned slags was undertaken to separate the two fractions, then just the fraction with particle size $> 750 \mu\text{m}$ was taken in this study (Fig.1). The chemical analysis of the two fractions by the XRF showed that the coarser fraction was rich in metallic aluminum (45.82%), aluminum oxide (33.18%), and aluminum hydroxide (17%) (Fig.1 b). The finer fraction was mainly aluminum oxide with a high content of impurities (MgAl_2O_4 (14%), CaCO_3 (16%), and SiO_2 (6%)). The taken fraction was characterized also by the XRD and the major constituents were found to be the aluminum compounds (Al , Al_2O_3 and $\text{Al}(\text{OH})_3$) with a small amount of magnesium aluminate (MgAl_2O_4) and calcite (CaCO_3) (see section 3.3).



Figure 1. Shape of the used aluminum slags

2.2. Methods

First, aluminum oxide was recovered as Al^{3+} ions by dissolving aluminum slags at various concentrations of H_2SO_4 (3, 5, 10, 15, 20, and 25%). The dissolution was carried out by putting 10 g of slag in a vial containing 100 ml of H_2SO_4 . The vial was placed on a hot plate to maintain the temperature of the mixture at $90 \pm 2 \text{ }^\circ\text{C}$. Then, the mixture was stirred continuously for 3 hours using a magnetic stirring bar. This allowed the three aluminum compounds (Al , $\text{Al}(\text{OH})_3$, and Al_2O_3) contained in the aluminum slag rock to react and dissolve in H_2SO_4 giving aluminum sulphates according to the following reactions [26]:



The obtained aluminum sulfates solution was separated from the solid residue by filtration using filter paper with a diameter of 0.2 μm . The obtained solution had an acidic pH between 1.5 and 2.5. A chemical precipitation was then carried out at 40 $^{\circ}\text{C}$ by adding a solution of NH_4OH (10%) drop wise [26, 27], increasing the solution pH up to 10 in order to obtain the optimal pH which corresponded to the maximum precipitation rate. The operation was followed by measuring the zeta potential of the different solutions to control the particle size and the precipitation rate as a function of pH. The gel that showed the maximum precipitation rate was filtered and washed with distilled water to remove the maximum impurities. This gel was then dried in an oven at 80 $^{\circ}\text{C}$ for 24 hours. Finally, the obtained powder was calcined in Nabertherm furnace at 1200 $^{\circ}\text{C}$ for 2 hours with a heating rate of 5 $^{\circ}\text{C}/\text{Min}$. Fig.2 is a summary diagram of the followed protocol.

2.3. Composition, microstructural and morphological characterizations

The chemical composition of the synthesized alumina powder was determined using the ZSX Primus IV wavelength dispersive X-Ray fluorescence spectrometer (WD-XRF), equipped with a 3/4 kW sealed X-ray tube that allowed the vacuum analysis from Be to U.

The crystallographic characterization of the phases existing in the used aluminum slags and in the synthesized alumina powder was done by Philips X'PERT Pro diffractometer equipped with a copper anti cathode ($\lambda = 1.54 \text{ \AA}$). The scanning angle 2θ was

between 5 and 80 $^{\circ}$ with a step interval of 0.017 $^{\circ}$.

For the FTIR analysis, the synthesized powder was compressed into cylindrical pellets, and then characterized by Perkin Elmer Fourier transform infrared spectrometer in the range of 400-4000 cm^{-1} at a resolution of 4 cm^{-1} .

The particle size, the zeta potential and the dispersion stability of particles inside the solution were measured at room temperature using Nano Partica SZ-100 nanoparticle analyzer. The electrophoretic light scattering (ELS) was the technique used for the ZP analysis.

The particle size of the synthesized alumina powder was also estimated in distilled water using HORIBA Partica LA-960 Laser Particle Size Analyzer.

The morphology of the synthesized powders was observed by the use of JEOL JSM-7001F scanning electron microscope (SEM) operating in high vacuum mode at an accelerating voltage of 15 kV.

3. Results and discussions

3.1. Effect of leaching acid concentration

In the present study, the concentration of leaching H_2SO_4 acid used to dissolve the aluminum slag rocks varied between 3 and 40%. Fig. 3 shows the percentage of alumina and sulphur trioxide in the recovered powder as a function of the concentration of leaching H_2SO_4 acid. As can be seen, the purity of the recovered alumina increased proportionally with the increase of the H_2SO_4 concentration to reach its maximum value (99.2%) at an optimal H_2SO_4 concentration of 15%. Beyond this acid concentration,

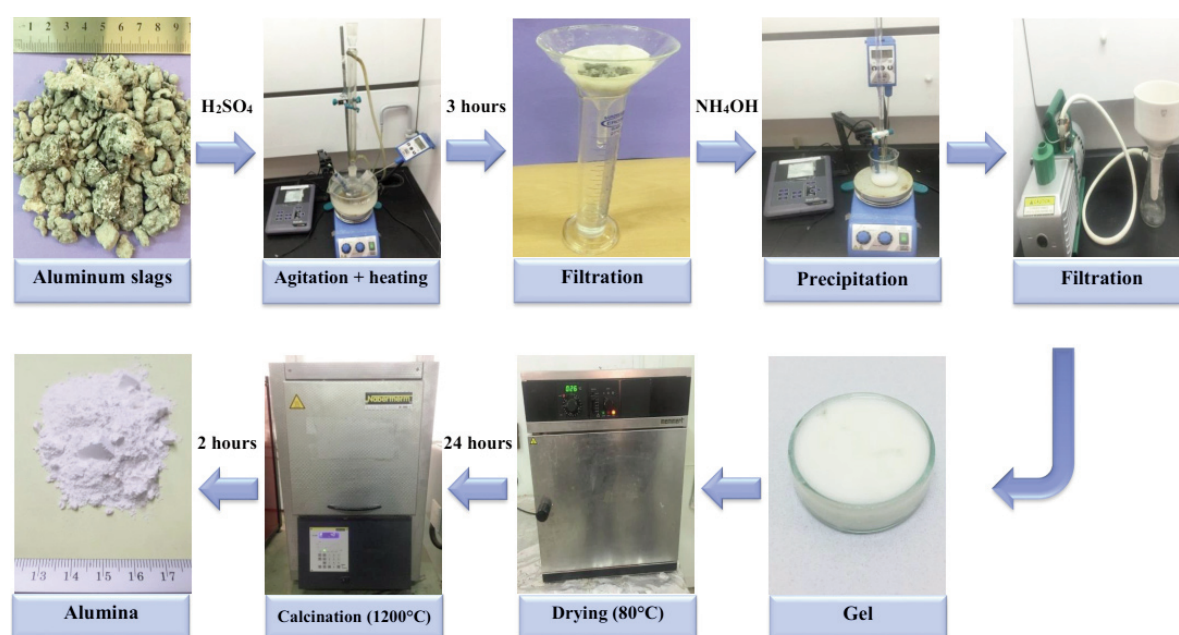


Figure 2. Summary diagram of the followed protocol



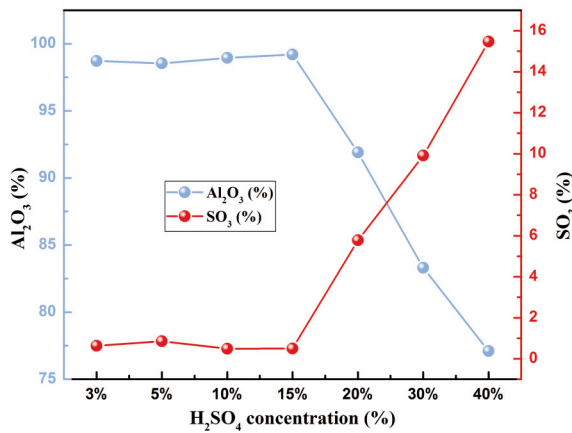


Figure 3. Alumina purity and SO₃ content vs. leaching acid concentration

the percentage of recovered alumina decreased with increasing acid concentration to reach a purity of 77.1% at an H₂SO₄ concentration of 40%. The slight increase in alumina percentage in the first stage was due to the increase of aluminum compounds solubility existing in the slag with increasing H₂SO₄ acid content (see equations 1-3). However, this solubility was limited at a concentration of acid solution [26], which was 15% in this study. Therefore, above a concentration of 15% H₂SO₄, the solubility of aluminum in the solution decreased. This resulted in an excess of sulfate anions (SO₄²⁻) that did not find enough Al³⁺ cations to completely transform into Al₂(SO₄)₃. These sulfate anions could not be removed in the precipitation phase. They remained in the precipitated gel and were converted to (SO₃) after calcination, resulting in a gradual decrease in the purity of the recovered powder with increasing H₂SO₄ concentration beyond 15%. It should be mentioned that the study of the purity of recovered alumina as a function of leaching acid concentration has not been addressed in other studies. However, the higher purity obtained in this study without any pretreatment of slags was comparable to the purity (99.28%) obtained by David et al. [28] using pretreated aluminum slags.

In the present study, the efficiency of alumina extraction process Q(%) was calculated according to the following relationship:

$$Q(\%) = \frac{Q_{Al \text{ extracted}}}{Q_{Al \text{ initiale}}} * 100\% \quad (4)$$

Where Q_{Al extracted} and Q_{Al initiale} are the quantity by gram of alumina in the extracted powder and the aluminum compounds in the slags, respectively. Fig. 4 represents the alumina extraction efficiency as a function of the leaching acid concentration. The efficiency of the extraction process increased from 74.12 to 93.75% as the leaching acid concentration

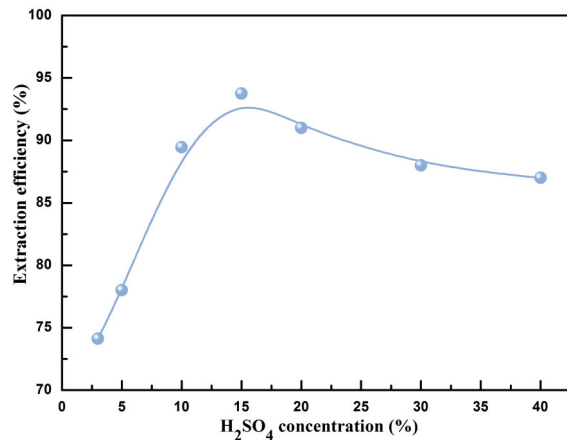


Figure 4. Efficiency of alumina extraction process vs. leaching acid concentration

was increased from 3 to 15%, and then decreased slightly to 87% when the acid concentration was increased from 15 to 40%. This confirmed the above results, indicating that the maximum dissolution of the aluminum compounds took place at an optimum acid concentration of 15%.

Table 1 provides a comparison of the extraction efficiency obtained in this study using the coarser fractions of aluminum slags with the results obtained from other studies using the finer fractions, under almost the same leaching experimental conditions. It can be seen that 15% H₂SO₄ acid concentration was also reported as the optimal concentration for the maximum alumina recovery in the studies provided by David et al. [26], Dash et al. [27], and Das et al. [28], in the case of non-pretreated slags. On the other hand, it was found that the aluminum slags fraction used in this work exhibited a higher extraction efficiency than that obtained in the mentioned studies. Only one study [27] found a higher efficiency than obtained in this study, but with the pretreatment of the slags and with the use of a relatively high leaching acid concentration of 50%. This indicated that the metallic aluminum-rich coarse fractions selected in the present study were more suitable in terms of efficiency for the alumina extraction than the oxide-rich fine fractions selected in the studies [26], [27], and [28].

3.2. Effect of the precipitation pH

The zeta potential is a measure that can provide us with information about the surface functionality, the stability of the dispersed particles, as well as interaction of dissolved compounds with the solid dispersed particles (catalysis). In this study, the zeta potential was monitored as a function of the precipitate pH during the drop wise addition of (NH₄OH) in order to control the particle size and

Table 1. Comparison of the obtained extraction efficiency with other studies

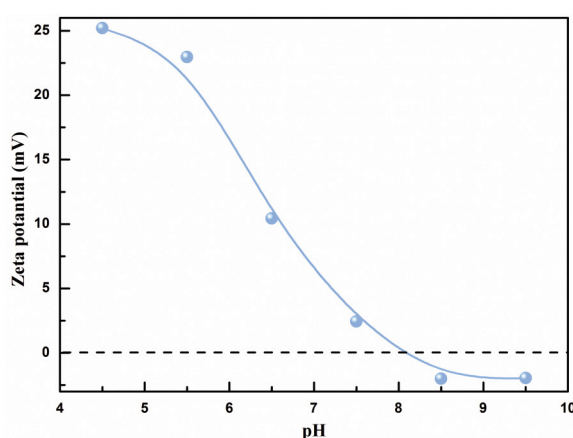
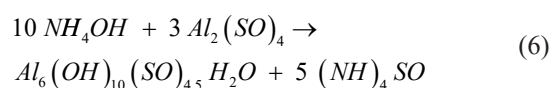
Raw material	Particle size	Optimal H ₂ SO ₄ leaching acid concentration	Efficiency of extraction	Temperature	Time	References
White coarser slags	>750 μm	15%	93.75% without pretreatment	90 °C	3 h	The present study
White finer slags	<850 μm	30 and 50%	85% without pretreatment and 95% with pretreatment	90 °C	1 h	[27]
White finer slags	<850 μm	30%	88% with pretreatment	90 °C	3 h	[26]
White finer slags	75 μm	15%	83.49% with pretreatment	90 °C	5 h	[28]

stability and to test the functionality and interactivity of the precipitated alumina surface. Fig. 5 shows the zeta potential of the prepared gel versus the pH value of the medium at ambient temperature. According to the figure, the zeta potential decreased meaningfully with increasing pH and took its negative values when the pH was higher than 8. While the isoelectric point, at which the surface acquired a net zero charge ($pZ = 0$ mV) was found at a pH_{zpc} (pH of zero potential charge) of about 8. According to [22, 29], the amphoteric equilibria can be represented by the following equation:



Thus, the precipitated alumina particles acquired a net negative charge in an aqueous medium at $pH > pH_{zpc}$ and a net positive charge at $pH < pH_{zpc}$. Furthermore, the pH_{zpc} value of about 8 for the recovered alumina was consistent with the range of 8 to 9.2 reported by [22, 29] for pure catalytic Al₂O₃ particles. This means that the alumina powders recovered from aluminum slags in this study may assume good catalytic-grade properties, which should be further verified in future studies by the measurement of particles surface area and porosity.

Fig. 6 shows the appearance of the Al₂(SO₄)₃ solution recovered after precipitation by NH₄OH at different pH values. It was clear that the pH value had a strong influence on the opacity of the solution and the rate of precipitation, where the solution became increasingly opaque as the pH has increased. The increase in the opacity of the solution was due to the increased rate of alumina precipitation as (Al₆(OH)₁₀(SO)₄·5H₂O) with the addition of NH₄OH according to the following reaction [18]:

**Figure 5.** Zeta potential of alumina precipitates at different pHs

Therefore, it was important to add the maximum possible amount of NH₄OH to achieve the maximum precipitation rate of alumina according to the equation (6). However, the precipitation of alumina reached its maximum rate when all Al³⁺ ions in the solution precipitated as (Al₆(OH)₁₀(SO)₄·5H₂O), that was what happened at a $pH >$ the neutralization pH between Al₂(SO₄)₃ acid and NH₄OH base, while a large increase in pH above the neutralization pH by the addition of NH₄OH did not result in further precipitation. It only offered an excess of NH₄OH and the solution was therefore diluted. This is why the pause to addition of ammoniac at a pH of 9.5, which was slightly higher than the neutralization pH, was preferred. This pH was considered to be optimal because it provided the higher opacity of the solution that correspond to the higher precipitation rate of alumina (Fig. 6).

The variation in the precipitation pH by adding NH₄OH always led to the formation of the same aluminum hydroxide phase, but with different morphologies (size and shape) [30, 31]. Fig. 7 shows the granulometric distribution of the precipitated

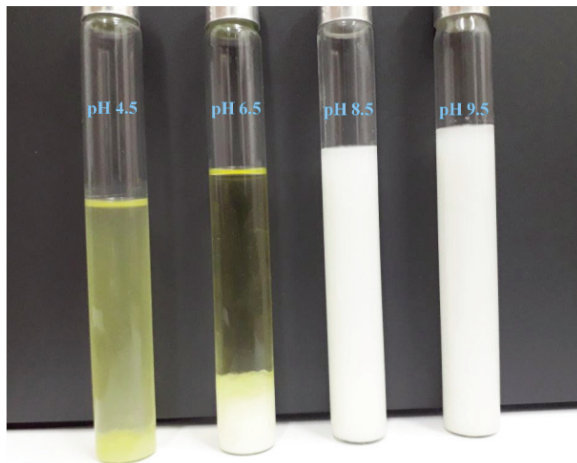


Figure 6. Effect of pH on the precipitation rate

alumina particles at different pH levels measured by the zetameter. It can be seen that there was an inversely relation between the precipitated alumina particle size and the medium pH, where the particles size decreased from 23 to 0.45 nm by raising the pH from 4.5 to 9.5. The obtaining of fine particle size in the suspension can lead to fine particles of the final recovered alumina powders. Therefore, it was necessary to choose the higher possible precipitation pH to obtain fine powders, but our process stopped at pH of 9.5, because, as it was shown previously, the large increase of the pH above the neutralization pH did not lead to any more alumina precipitation.

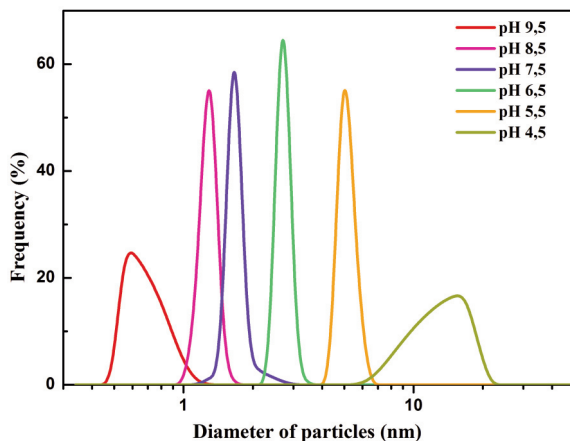


Figure 7. Granulometric distribution of alumina precipitates produced at different pH levels

3.3. Microstructural and morphological characteristics of the recovered alumina

The aluminum hydroxide powder obtained after the drying of the precipitated gel at 80 °C presented an amorphous structure [13, 26]. This powder was calcined at 1200°C for dehydroxylation and

desulfurization. During this calcination, a crystallization and some phase transformations were also performed. The XRD spectrum of the alumina powder obtained after the calcination is shown in Fig. 8. The intense and sharp diffraction peaks indicated

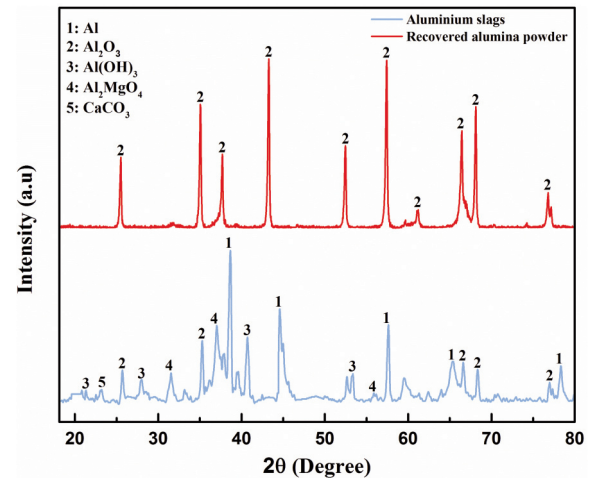


Figure 8. XRD patterns of the used aluminum slags and the recovered alumina powder

that the obtained powder was of high crystallinity. Moreover, in comparison with the spectrum of aluminum slags, the peaks of aluminum (Al), aluminum hydroxide ($\text{Al}(\text{OH})_3$), magnesium aluminate (Al_2MgO_4), and calcite (CaCO_3) disappeared. The disappearance of these peaks indicated that the extracted alumina was of high purity. It also indicated that the chemical process used in this work was effective in extracting and recovering almost all of the aluminum (Al) contained in the slags in the form of alumina (Al_2O_3). On the other hand, the comparison of the XRD pattern of the synthesized alumina with the international database (ICDD) showed that the latter was a single corundum phase ($\alpha\text{-Al}_2\text{O}_3$) (ICSD 01-081-1667 [32]). Similar observations were also made in previous studies by the calcination of aluminum hydroxide powders at the same temperature of 1200 °C [13, 26, 31]. However, the use of lower calcination temperatures in some other studies has led to the recovery of other alumina phases from aluminum slags, such as γ -alumina at 600 °C [22], η -alumina at 900 °C [26], $\alpha+\eta$ alumina at 1000 °C [13], and $\alpha+\gamma$ alumina at 1050 °C [28]. This means that the appropriate structure can be obtained for any application by simply changing the calcination temperature. In this study, the focus was only on the most stable polymorph α -alumina, which could be used in a wide range of applications especially at high temperatures.

The Fourier transform infrared analysis (FTIR) of the synthesized alumina powder in the region of wave numbers 400–4000 cm^{-1} is shown in Fig. 9. A peak

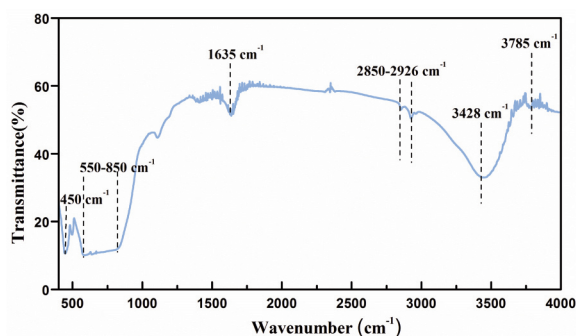


Figure 9. FTIR spectra of the alumina powder calcined at 1200 °C

observed at around 450 cm^{-1} may be due to Al–O bending vibrations in the AlO_6 octahedral units [1, 13]. An intense and broad absorption peak due to the stretching Al–O modes was also found in the range of 550 to 850 cm^{-1} [13, 33–35]. The absorption band at 1635 cm^{-1} was due to the bending vibrations of H–O–H bonds in the hydration water [29], where the residual traces related to water were due to hygroscopic nature of the KBr pellets employed as mounting material [13]. The bands observed around 2845, 2926, 3428, and 3785 cm^{-1} were due to the stretching vibration of –O–H. It is quite possible that this effect occurred due to the moisture adsorbed on the surface of the synthesized powders [13, 36]. A consolidated list of the wave numbers and the attribution of bands of the calcined powder was given in Table 2. The FTIR result may account for the approximated chemical composition $[\text{AlO}_x(\text{OH})_y\text{zH}_2\text{O}]$ for the surface of the synthesized $\alpha\text{-Al}_2\text{O}_3$. This surface composition was similar to those suggested for partially dehydroxylated Al_2O_3 surfaces [29]. Hence, the FTIR spectrum of the extracted $\alpha\text{-Al}_2\text{O}_3$

Table 2. Attribution of the bands of the calcined alumina powder vs. the wave number

Wave number (cm^{-1})	Attribution
2850, 2926, 3428 and 3785	$\nu(\text{O-H})$
1635	$\delta(\text{H-O-H})$
550-850	$\nu(\text{Al-O})$
450	$\delta(\text{Al-O})$

Al_2O_3 indicated that they exposed largely clean surfaces constituting aluminum oxide and hydroxide, as well as H_2O molecules. Moreover, no clear peaks of sulfur or carbon contaminants found to be on their surface.

Fig. 10 (a) shows the particle size distribution of the synthesized alumina powder measured by laser diffraction particle sizing method. As it can be seen, the recovered alumina showed a wide particles size distribution that ranged from 40 nm to 20 μm . The bimodal character of the particle size distribution was very clear in the size distribution curve. Two peaks were found corresponding to two populations, the first one lower than 0.6 μm and the second one higher than 0.6 μm . The observation of the synthesized powder by the SEM (Fig. 11) showed that the coarse fractions ($\geq 0.6 \mu\text{m}$) were due to the agglomeration of the small particles ($\leq 0.6 \mu\text{m}$), which was due to the high energy of $\alpha\text{-Al}_2\text{O}_3$ nanoparticles surfaces thermodynamically unstable at room temperature [37]. This agglomeration was mainly insured by the weak hydrogen-type bonds between the small particles due to the presence of (OH) groups on the particles surfaces as shown in the FTIR results (Fig. 9). By the use of the cumulative presentation of the particle size (Fig. 10 (b)), it can be seen clearly that about 51% of

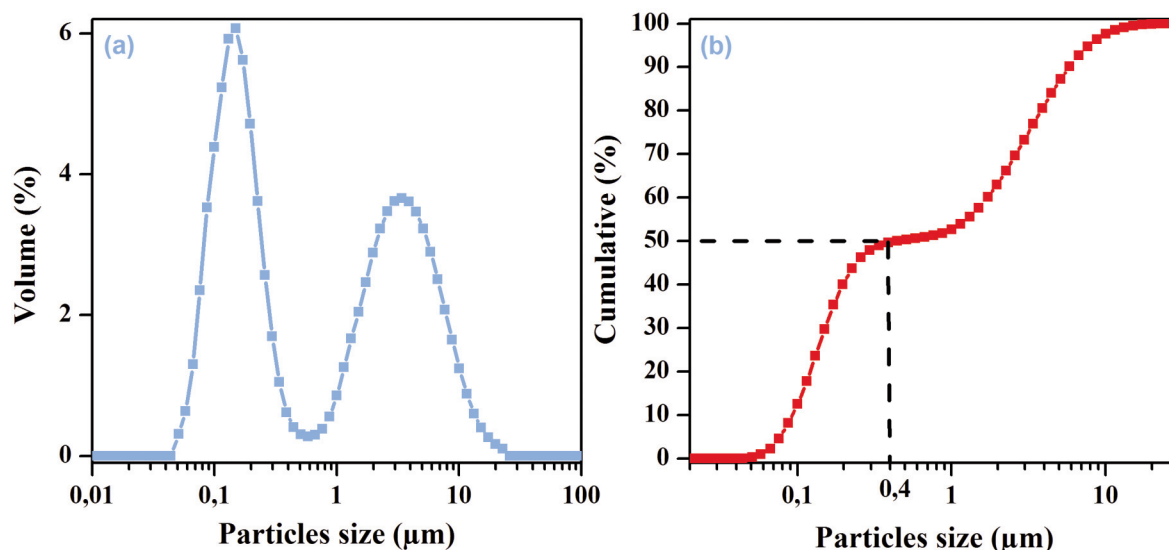


Figure 10. The particle size distribution of the synthesized powder

the particles were smaller than 0.6 μm and the remaining 49% were larger than 0.6 μm , while the average particle size (d_{50}) of the grains was found to be in the order of 400 nm. This large particle size distribution tends to maximize particle packing density, where the large particles can form a rigid structure, and the fine active particles form the matrix and bind the large particles after sintering, which is very suitable for certain applications such as refractory materials [17] and electrode-coated for lithium-ion batteries [38]. It is worth noting that some applications like catalysis, abrasives and nanocomposites need to disperse fine α -alumina particles with narrow particle size distribution [37]. However, this alumina powder grade can be obtained easily using the recovered alumina through many methods like sieving [39], supersonic vibration [40], or by the selective corrosion and refined fractionated coagulation separation [37].

The morphology and the chemical composition of the recovered α -alumina powders are of great importance because they can have a considerable impact on the microstructure, catalytic sensitivity and mechanical behavior of the elaborated materials [6]. In agreement with laser diffraction particle sizing results, the SEM observation of the synthesized α -alumina in Fig. 11 showed a wide particle size distribution, with particles sizes ranging from

submicron to tens of micrometers. The individual α - Al_2O_3 particles had almost a morphology of short whiskers with irregular ends, each approximately 1 μm in average length and 0.2 μm in average diameter. These submicronic whiskers tended to stick together to form micro-particles. As a result, the synthesized α - Al_2O_3 powder showed a bimodal distribution nature as shown in Fig. 11. It should be mentioned that other morphologies of α - Al_2O_3 extracted from aluminum slags could be obtained, such as the spherical morphology [41] or the irregular morphology [28]. These differences in the morphology were mainly due to the differences in the used products and experimental protocol (pH, temperature, type, and concentration of leaching acids, etc.). The atomic composition of the recovered α - Al_2O_3 powder was also analyzed by the EDS, which revealed the presence of high amount of Al and O (99.59 at.%) with very small amounts of impurities confirming the high purity of the recovered alumina (Fig. 11 (d)).

4. Conclusions

The objective of this study was to treat aluminum slags in order to eliminate their environmental threat and to exploit them in the extraction of high value-added alumina. A controllable acid leaching technique

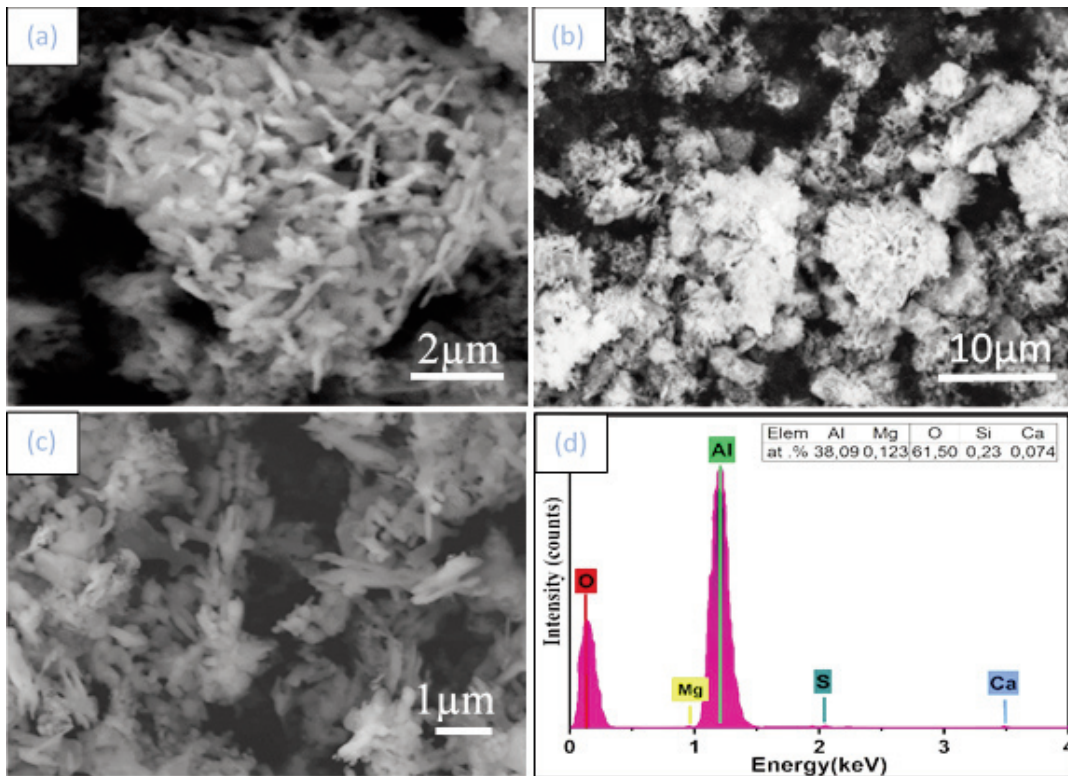


Figure 11. SEM micrograph of the recovered alumina powder with different magnifications (a) (b) (c) and the composition of the recovered powder (d)

followed by precipitation was used for the extraction. The following important conclusions can be drawn from this study:

(1) The coarser aluminum-rich fractions of the slags used in this study were found to be technically more suitable for alumina extraction, compared to the finer oxides-rich fractions used in other studies.

(2) A high purity of recovered alumina (99.2%) and a highest extraction efficiency (93.75%) were achieved at an optimum leaching H_2SO_4 concentration of 15%.

(3) The XRD analysis revealed that the recovered alumina was a pure and high crystalline corundum (α -alumina).

(4) The FTIR spectrum of the extracted α - Al_2O_3 indicated that it exposed largely clean surfaces, with no clear signs of undesirable contaminants.

(5) The granulometric analysis of the produced alumina showed a bi-modal character of the particle size distribution, ranging from 40 nm to 20 μm .

(6) The SEM observation of the synthesized α -alumina showed that the individual α - Al_2O_3 particles had almost a short submicron whiskers morphology.

(7) The above properties of the recovered alumina powder allowed it to be used in the most common applications of α -alumina.

Author Contributions

The authors confirm their contribution to the paper as follows: Study conception and design: A. Benkhelif and M. Kollı; Analysis and interpretation of results: A. Benkhelif and M. Hamidouche; Draft manuscript preparation: A. Benkhelif, M. Hamidouche and M. Kollı. All authors reviewed the results and approved the final version of the manuscript.

Data Availability Statement

The authors confirm that the data supporting the results of this study are available within the article. Any additional data can be provided upon request from the corresponding author [M. Hamidouche].

Conflicts of Interest

The authors declare that no conflicts of interest to disclose.

References

- [1] X. Su, J. Li, Low temperature synthesis of single-crystal alpha alumina platelets by calcining bayerite and potassium sulfate, *Journal of Materials Science & Technology*, 27 (11) (2011) 1011–1015. [https://doi.org/10.1016/S1005-0302\(11\)60179-5](https://doi.org/10.1016/S1005-0302(11)60179-5)
- [2] Y. Huang, Y. Xia, Q. Long, S. Liao, Y. Li, J. Liang, J. Cai, Large-scale synthesis of aluminum borate nanowires by a simple molten salt method, *Ceramics International*, 41(2) (2015) 2607–2610. <https://doi.org/10.1016/j.ceramint.2014.10.012>
- [3] G. Feng, W. Jiang, J. Liu, C. Li, Q. Zhang, L. Miao, Q. Wu, Novel nonaqueous precipitation synthesis of alumina powders, *Ceramics International*, 43 (16) (2017) 13461–13468. <https://doi.org/10.1016/j.ceramint.2017.07.050>
- [4] L. Liu, X. Zhang, L. Zhu, Y. Wei, C. Guo, H. Li, Preparation of hexagonal micro-sized α - Al_2O_3 platelets from a milled $Al(OH)_3$ precursor with NH_4F and NH_4Cl additives, *Zeitschrift für Naturforschung B*, 74 (7-8) (2019) 579–583. <https://doi.org/10.1515/znB-2019-0080>
- [5] S.H. Lim, K.Y. Zeng, C.B. He, Morphology, tensile and fracture characteristics of epoxy - alumina nanocomposites, *Materials Science and Engineering: A*, 527 (21-22) (2010) 5670–5676. <https://doi.org/10.1016/j.msea.2010.05.038>
- [6] W.L. Suchanek, J.M. Garces, P.F. Fulvio, M. Jaroniec, Hydrothermal synthesis and surface characteristics of novel alpha alumina nanosheets with controlled chemical composition, *Chemistry of Materials*, 22 (24) (2010) 6564–6574. <https://doi.org/10.1021/cm102158w>
- [7] G. Paglia, C.E. Buckley, A.L. Rohl, R.D. Hart, K. Winter, A.J. Studer, B.A. Hunter, J.V. Hanna, Boehmite derived γ -alumina system. 1. Structural evolution with temperature, with the identification and structural determination of a new transition phase, γ' -alumina, *Chemistry of Materials*, 16 (2) (2004) 220–236. <https://doi.org/10.1021/cm034917j>
- [8] Y. Wang, J. Wang, M. Shen, W. Wang, Synthesis and properties of thermostable γ -alumina prepared by hydrolysis of phosphide aluminum, *Journal of Alloys and Compounds*, 467 (1-2) (2009) 405–412. <https://doi.org/10.1016/j.jallcom.2007.12.007>
- [9] G.P. Johnston, R. Muenchausen, D.M. Smith, W. Fahrenholtz, S. Foltyn, Reactive laser ablation synthesis of nanosize alumina powder, *Journal of the American Ceramic Society*, 75 (12) (1992) 3293–3298. <https://doi.org/10.1111/j.1151-2916.1992.tb04424.x>
- [10] T. Ogihara, H. Nakajima, T. Yanagawa, N. Ogata, K. Yoshida, N. Matsushita, Preparation of monodisperse, spherical alumina powders from alkoxides, *Journal of the American Ceramic Society*, 74 (9) (1991) 2263–2269. <https://doi.org/10.1111/j.1151-2916.1991.tb08294>
- [11] E. Kato, K. Daemon, M. Nanbu, Decomposition of two aluminum sulfates and characterization of the resultant aluminas, *Journal of the American Ceramic Society*, 64 (8) (1981) 436–443. <https://doi.org/10.1111/j.1151-2916.1981.tb09892>
- [12] H. Noda, K. Muramoto, H. Kim, Preparation of nano-structured ceramics using nanosized Al_2O_3 particles, *Journal of Materials Science*, 38 (9) (2003) 2043–2047. <https://doi.org/10.1023/A:1023553925110>
- [13] I.N. Bhattacharya, P.K. Gochhayat, P.S. Mukherjee, S. Paul, P.K. Mitra, Thermal decomposition of precipitated low bulk density basic aluminium sulfate, *Materials Chemistry and Physics*, 88 (1) (2004) 32–40. <https://doi.org/10.1016/j.matchemphys.2004.04.024>
- [14] M.C. Shinzato, R. Hypolito, Solid waste from aluminum recycling process: characterization and reuse of its economically valuable constituents, *Waste Management*, 25 (1) (2005) 37–46. <https://doi.org/10.1016/j.wasman.2004.08.005>



- [15] P.E. Tsakiridis, Aluminium salt slag characterization and utilization—A review, *Journal of Hazardous Materials*, 217 (1) (2012) 1–10. <https://doi.org/10.1016/j.jhazmat.2012.03.052>
- [16] S.O. Adeosun, O.I. Sekunowo, O.O. Taiwo, W.A. Ayoola, A. Machado, Physical and Mechanical Properties of Aluminum Dross, *Advances in Materials*, 3 (2) (2014) 6. <https://doi.org/10.11648/j.am.20140302.11>
- [17] A. Gil, S.A. Korili, Management and valorization of aluminum saline slags: Current status and future trends, *Chemical Engineering Journal*, 289 (1) (2016) 74–84. <https://doi.org/10.1016/j.cej.2015.12.069>
- [18] A. Meshram, K.K. Singh, Recovery of valuable products from hazardous aluminum dross: A review, *Resources, Conservation and Recycling*, 130 (1) (2018) 95–108. <https://doi.org/10.1016/j.resconrec.2017.11.026>
- [19] T. Hiraki, A. Nosaka, N. Okinaka, T. Akiyama, Synthesis of zeolite-X from waste metals, *ISIJ International*, 49 (10) (2009) 1644–1648. <https://doi.org/10.2355/isijinternational.49.1644>
- [20] S. Sangita, N. Nayak, C.R. Panda, Extraction of aluminium as aluminium sulphate from thermal power plant fly ashes, *Transactions of Nonferrous Metals Society of China*, 27 (9) (2017) 2082–2089. [https://doi.org/10.1016/S1003-6326\(17\)60231-0](https://doi.org/10.1016/S1003-6326(17)60231-0)
- [21] F.H. Kamil, A. Salmiaton, R.M.H.R. Shahruzzaman, R. Omar, A.G. Alsultsan, Characterization and application of aluminum dross as catalyst in pyrolysis of waste cooking oil, *Bulletin of Chemical Reaction Engineering*, 12 (1) (2017) 81–88. <https://doi.org/10.9767/bcrec.12.1.557.81-88>
- [22] E.A. El-Katatny, S.A. Halawy, M.A. Mohamed, M.I. Zaki, Surface composition, charge and texture of active alumina powders recovered from aluminum dross tailings chemical waste, *Powder Technology*, 132 (2-3) (2003) 137–144. [https://doi.org/10.1016/S0032-5910\(03\)00047-0](https://doi.org/10.1016/S0032-5910(03)00047-0)
- [23] M.S. Reddy, D. Neeraja, Aluminum residue waste for possible utilisation as a material: a review, *Indian Academy of Sciences*, 43 (8) (2018) 124. <https://doi.org/10.1007/s12046-018-0866-2>
- [24] M.S.R. Sarker, M.Z. Alam, M.R. Qadir, M.A. Gafur, M. Moniruzzaman, Extraction and characterization of alumina nanopowders from aluminum dross by acid dissolution process, *International Journal of Minerals, Metallurgy and Materials*, 22 (4) (2015) 429–436. <https://doi.org/10.1007/s12613-015-1090-2>
- [25] T. Hiraki, T. Miki, K. Nakajima, K. Matsubae, S. Nakamura, T. Nagasaka, Thermodynamic analysis for the refining ability of salt flux for aluminum recycling, *Materials*, 7 (8) (2014) 5543–5553. <https://doi.org/10.3390/ma7085543>
- [26] B.R. Das, B. Dash, B.C. Tripathy, I.N. Bhattacharya, S.C. Das, Production of η -alumina from waste aluminium dross, *Minerals Engineering*, 20 (3) (2007) 252–258. <https://doi.org/10.1016/j.mineng.2006.09.002>
- [27] B. Dash, B.C. Tripathy, I.N. Bhattacharya, T. Subbaiah, A comparative study on the precipitation of hydrated alumina from different sources, *International Journal of Metallurgical Engineering*, 1 (1) (2012) 78–82. <https://doi.org/10.5923/j.ijmeee.20120105.02>
- [28] E. David, J. Kopac, Aluminum recovery as a product with high added value using aluminum hazardous waste, *Journal of Hazardous Materials*, 261 (1) (2013) 316–324. <https://doi.org/10.1016/j.jhazmat.2013.07.042>
- [29] M. Mahinroosta, A. Allahverdi, A promising green process for synthesis of high purity activated-alumina nanopowder from secondary aluminum dross, *Journal of Cleaner Production*, 179 (1) (2018) 93–102. <https://doi.org/10.1016/j.jclepro.2018.01.079>
- [30] F. Karouia, Traitement thermique de boehmite de taille et forme de particules contrôlées: vers l'optimisation des propriétés de l'alumine gamma, PhD Thesis, Toulouse III-Paul Sabatier University, 2014.
- [31] H. Zhang, D. Zhu, S. Grasso, C. Hu, Tunable morphology of aluminum oxide whiskers grown by hydrothermal method, *Ceramics International*, 44 (13) (2018) 14967–14973. <https://doi.org/10.1016/j.ceramint.2018.05.072>
- [32] A.S. Brown, M.A. Spackman, R.J. Hill, The electron distribution in corundum. A study of the utility of merging single-crystal and powder diffraction data, *Acta Crystallographica Section A*, 49 (3) (1993) 513–527. <https://doi.org/10.1107/S0108767392011267>
- [33] J. Shah, M. Ranjan, V. Davariya, S.K. Gupta, Y. Sonvane, Temperature-dependent thermal conductivity and viscosity of synthesized α -alumina nanofluids, *Applied Nanoscience*, 7 (8) (2017) 803–813. <https://doi.org/10.1007/s13204-017-0594-7>
- [34] K.C. Song, S.E. Pratsinis, The effect of alcohol solvents on the porosity and phase composition of titania, *Journal of Colloid and Interface Science*, 231 (2) (2000) 289–298. <https://doi.org/10.1006/jcis.2000.7147>
- [35] J.K. Pradhan, I.N. Bhattacharya, S.C. Das, R.P. Das, R.K. Panda, Characterisation of fine polycrystals of metastable η -alumina obtained through a wet chemical precursor synthesis, *Materials Science and Engineering: B*, 77 (2) (2000) 185–192. [https://doi.org/10.1016/S0921-5107\(00\)00486-4](https://doi.org/10.1016/S0921-5107(00)00486-4)
- [36] J.S. Lee, H.S. Kim, N.-K. Park, T.J. Lee, M. Kang, Low temperature synthesis of α -alumina from aluminum hydroxide hydrothermally synthesized using $[\text{Al}(\text{C}_2\text{O}_4)_2(\text{OH})_2]$ complexes, *Chemical Engineering Journal*, 230 (1) (2013) 351–360. <https://doi.org/10.1016/j.cej.2013.06.099>
- [37] S. Pu, L. Li, J. Ma, F. Lu, J. Li, Disperse fine equiaxed alpha alumina nanoparticles with narrow size distribution synthesised by selective corrosion and coagulation separation, *Scientific Reports*, 5 (1) (2015) 11575. <https://doi.org/10.1038/srep11575>
- [38] N. Kanhere, K. Rafiz, G. Sharma, Z. Sun, Y. Jin, Y.S. Lin, Electrode-coated alumina separators for lithium-ion batteries-effect of particle size and distribution of alumina powders, *Powder Technology*, 353 (1) (2019) 230–237. <https://doi.org/10.1016/j.powtec.2019.05.007>
- [39] K. Nakahira, T. Hotta, M. Naito, N. Shinohara, Y. Cho, S. Katori, H. Emoto, T. Yamada, T. Takahashi, M. Okumiya, Characterization of coarse particles in alumina powders by a wet sieving method, *Journal of the European Ceramic Society*, 23 (10) (2003) 1661–1666. [https://doi.org/10.1016/S0955-2219\(02\)00361-8](https://doi.org/10.1016/S0955-2219(02)00361-8)
- [40] C.J. Papini, W.K. Yoshito, D. Gouvêa, R.M.L. Neto, Particle size distribution analysis of an alumina



powder: influence of some dispersants, pH and supersonic vibration, Materials Science Forum, (498-499) (2005)73–78.
<https://doi.org/10.4028/www.scientific.net/MSF.498-499.73>

[41] M. Mahinroosta, A. Allahverdi, Hazardous aluminum dross characterization and recycling strategies: A critical review, Journal of Environmental Management, 223 (1) (2018) 452–468.
<https://doi.org/10.1016/j.jenvman.2018.06.068>

SINTEZA SUBMIKRONSKE α -GLINICE IZ ALUMINIJUMSKE ŠLJAKE

A. Benkhelif ^{a,b}, M. Kolli ^{a,b}, M. Hamidouche ^{a,b,c,*}

^a Univerzitet Ferhat Abbas u Setifu, Odsek za istraživanje materijala, Setif, Alžir

^b Univerzitet Ferhat Abbas u Setifu, Institut za optiku i preciznu mehaniku, Setif, Alžir

^c Istraživački centar za industrijsku tehnologiju CRTI, B.P. 64, Čeraga 16014, Alžir

Apstrakt

U ovom radu je submikronska α -glinica velike vrednosti uspešno dobijena iz aluminijumske šljake nastale u lokalnoj industriji aluminijuma. Tehnika ekstrakcije se zasnivala na luženju šljake u prisustvu H_2SO_4 koje je praćeno precipitacijom. Tokom istraživanja korišćene su grublje frakcije šljake bogate aluminijumom umesto finijih frakcija bogatih oksidima koje su se obično koristile u prethodnim istraživanjima. Taloženje šljake lužene u prisustvu NH_4OH je kontrolisano zetametrom kako bi odredila optimalna pH vrednost taloženja. Nakon toga, dobijeni gel koji je pokazivao veću stopu precipitacije i imao sitniju veličinu čestica, kalcinisan je na 1200 °C, a zatim su određene njegove karakteristike pomoću XRF, XRD, FTIR, SEM, EDS i laserske granulometrije. Čak i bez prethodnog tretmana šljake, XRF analiza je pokazala da se visoka čistoća i efikasnost ekstrakcije od 99,2%, odnosno 93,75%, mogu postići kada je koncentracija kiseline korišćene za luženje samo 15%. XRD spektar je pokazao da dobijena glinica predstavlja čist α -korund, što je potvrđeno FTIR spektrom koji je ukazao na postojanje samo Al-O veze. Laserska granulometrija je ukazala na činjenicu da je dobijeni prah pokazao široku distribuciju veličine čestica, koja je iznosila između 50 nm i 20 μ m, dok je prosečna veličina čestica (d_{50}) bila oko 400 nm. SEM analiza je otkrila da su zrna bila u obliku submikronskih vlati. Prethodno navedene analize su omogućile da ovaj dobijeni prah glinice ima standardnu primenu, kao što je primena za postizanje vatrostalnosti, za keramička vlakna, abrazivna sredstva, itd. Dobijeni prah takođe može imati primenu kao termički stabilna zamena za prah glinice koji se obično koristi, što zahteva dalja istraživanja u budućnosti.

Ključne reči: α -glinica; Aluminijumska šljaka; Luženje u kiselim rastvorima; Precipitacija; Kalcinacija.

